Received: 31 March 2023 | Revised: 4 July 2023 | Accepted: 20 July 2023

DOI: 10.1111/ejn.16107

SPECIAL ISSUE ARTICLE

EJN European Journal of Neuroscience FENS WILEY

Neurophysiological and Neuroimaging Phenotypes in Schizophrenia Spectrum Disorders

Is source-resolved magnetoencephalographic mismatch negativity a viable biomarker for early psychosis?

Fran López-Caballero | **Mark Curtis** | **Brian A. Coffman** | **Dean F. Salisbury**

Clinical Neurophysiology Research Laboratory, Western Psychiatric Hospital, University of Pittsburgh School of Medicine, Pittsburgh, Pennsylvania, USA

Correspondence
Dean F. Salisbury, Clinical Neurophysiology Research Laboratory, Western Psychiatric Hospital, University of Pittsburgh School of Medicine, 3501 Forbes Ave, Suite 420, Pittsburgh 15213, PA, USA.
Email: salisburyd@upmc.edu

Funding information
National Institutes of Health, Grant/Award Numbers: MH113533, R01 MH108568

Edited by: John Foxe

Abstract

Mismatch negativity (MMN) is an auditory event-related response reflecting the pre-attentive detection of novel stimuli and is a biomarker of cortical dysfunction in schizophrenia (SZ). MMN to pitch (pMMN) and to duration (dMMN) deviant stimuli are impaired in chronic SZ, but it is less clear if MMN is reduced in first-episode SZ, with inconsistent findings in scalp-level EEG studies. Here, we investigated the neural generators of pMMN and dMMN with MEG recordings in 26 first-episode schizophrenia spectrum (FE_{sz}) and 26 matched healthy controls (C). We projected MEG inverse solutions into precise functionally meaningful auditory cortex areas. MEG-derived MMN sources were in bilateral primary auditory cortex (A1) and belt areas. In A1, pMMN FE_{sz} reduction showed a trend towards statistical significance ($F_{(1,50)} = 3.31$; $p = .07$), and dMMN was reduced in FE_{sz} ($F_{(1,50)} = 4.11$; $p = .04$). Hypothesis-driven comparisons at each hemisphere revealed dMMN reduction in FE_{sz} occurred in the left ($t_{(56)} = 2.23$; $p = .03$; $d = .61$) but not right ($t_{(56)} = 1.02$; $p = .31$; $d = .28$) hemisphere, with a moderate effect size. The added precision of MEG source solution with high-resolution MRI and parcellation of A1 may be requisite to detect the emerging pathophysiology and indicates a critical role for left hemisphere pathology at psychosis onset. However, the moderate effect size in left A1, albeit larger than reported in scalp MMN meta-analyses, casts doubt on the clinical utility of MMN for differential diagnosis, as a majority of patients will overlap with the healthy individual's distribution.

KEYWORDS
duration, first-episode, pitch, schizophrenia, source solutions

Abbreviations: CPZmed, chlorpromazine-equivalent dose; C, controls; dMMN, duration MMN; ECG, electrocardiogram; EEG, electroencephalography; FDR, false discovery rate; FE, first-episode; FEP, first-episode psychosis; FE_{Aff}, first-episode affective; FE_{sz}, first-episode schizophrenia; fMRI, functional magnetic resonance imaging; HPI, head position indicator; HCP-MMP, Human Connectome Project multimodal parcellation; LBelt, lateral belt; MRI, magnetic resonance imaging; MEG, magnetoencephalography; MCCB, MATRICS Consensus Cognitive Battery; MBelt, medial belt; MED2SCAN, medication to scan; MMN, mismatch negativity; MNI, Montreal Neurological Institute; SZ, schizophrenia; PBelt, parabelt; PSES, parental socio-economic status; pMMN, pitch MMN; PANSS, Positive and Negative Syndrome Scale; PSYCH2SCAN, psychosis onset to scan; SES, socio-economic status; WASI, Wechsler Abbreviated Scale of Intelligence.

[Correction added on 24 April 2024, after first online publication: The Special Issue title has been corrected for this article.]

1 | INTRODUCTION

Mismatch negativity (MMN) is an event-related potential/field elicited by infrequent stimuli breaking a regular sound sequence (Näätänen et al., 1978, 2007). It can be recorded with electroencephalography (EEG) or magnetoencephalography (MEG) and is typically obtained by presenting a series of standard repetitive sounds occasionally interrupted by deviants differing in one or more dimensions (e.g. intensity, pitch, duration). There is debate as to whether MMN reflects an active comparison of incoming stimuli with a memory trace of past events (Näätänen, 1990), a prediction error signal to update our internal models (Winkler, 2007) or the passive sensory adaptation to repetitive stimuli contrasting with non-adapted responses to rare deviants (May & Tiitinen, 2010). Nonetheless, MMN is consistently impaired in chronic schizophrenia (SZ) (Erickson et al., 2016; Haigh et al., 2017; Light & Näätänen, 2013; Salisbury et al., 2002; Shelley et al., 1991; Umbricht & Krljes, 2005) and holds potential clinical utility due to its associations with several core features of the disease, such as cortical structural abnormalities (Curtis et al., 2021; Rasser et al., 2011; Rissling et al., 2014; Salisbury et al., 2007, 2020), impaired neuroreceptor function (NMDA; Javitt et al., 1996) and impoverished social functioning (Light & Braff, 2005; Murphy et al., 2020; Wynn et al., 2010), among others (Todd et al., 2013).

While MMN is severely reduced in long-term SZ, with large effect sizes (Cohen's $d > 1$; Umbricht & Krljes, 2005 or 0.8; Erickson et al., 2016; Haigh et al., 2017), it is unclear if it is impaired during the first-episode (FE) phase of the disease. Some studies report pitch (pMMN) (Todd et al., 2022) and duration MMN (dMMN) (Hermens et al., 2010; Higuchi et al., 2013) reductions in FE, while some others do not (pMMN: Magno et al., 2008; Salisbury et al., 2002; Valkonen-Korhonen et al., 2003; dMMN: Murphy et al., 2020; Salisbury et al., 2017). Meta-analyses support that MMN is much less reduced in FE (Erickson et al., 2016; Haigh et al., 2017), with negligible effect sizes for pMMN ($d = .04$) and small-to-moderate for dMMN ($d = .47$) (Haigh et al., 2017). Antipsychotic medication (Haigh et al., 2017) and premorbid intelligence quotient (IQ) (Salisbury et al., 2017) were suggested as potential confounds contributing to the discrepancies among FE MMN studies. These discrepancies also fuel the debate as to whether or not MMN should be considered a biomarker for the early identification of the disease (e.g. in clinical at-risk individuals: Atkinson et al., 2012; Näätänen et al., 2016). Some studies suggest that, rather than a biomarker for disease presence, MMN serves better as a biomarker of disease progression (Erickson et al., 2017; Magno et al., 2008; Salisbury et al., 2007; Todd et al., 2008). Supporting this view, MMN impairment, particularly in pMMN, worsens as the disease progresses, with most of the reduction occurring within the first 2 years after psychosis onset (Devrim-Üçok et al., 2008; Salisbury et al., 2007).

Progressive grey matter loss in schizophrenia follows a similar time course as MMN reduction, starting early in the disorder and rapidly declining over the first few years, particularly over temporal and frontal cortices (Cropley et al., 2017; Hirayasu et al., 1998; Kasai et al., 2003; Thompson et al., 2001). Correlations between pMMN and left auditory cortex volumes were observed in FE at first hospitalization (Salisbury et al., 2007), and, in both pMMN and dMMN, within 2 months of first clinical contact for psychosis (Curtis et al., 2021; Salisbury et al., 2020). This led to the hypothesis that MMN deficits emerge as a consequence of grey matter loss in its neural generators that starts before disease onset (Salisbury et al., 2007). Other potentially overlapping and interdependent factors contributing to MMN deficits in FE and SZ may include (1) reductions in dendritic spine density and mean somal volume of pyramidal cells in the auditory cortex (Sweet et al., 2009), (2) impaired network connectivity between frontal and auditory areas (Alho et al., 1994), (3) altered NMDA receptor function (Javitt et al., 1996) and (4) misattribution of salience to deviant stimuli (Todd et al., 2012).

To further disentangle the complex pathophysiology behind MMN deficits in SZ, it is crucial to establish the precise structural and functional alterations close to disease onset. Current knowledge of MMN reduction in FE relies primarily on EEG scalp-derived responses with limited spatial resolution. Only a few studies used EEG dipole fitting-based analysis in FE MMN research. Oades et al. (2006) found reduced sources in temporal lobes and different source locations for controls and FE, while in Randau et al. (2019), MMN reductions were specifically located in the right superior temporal gyrus (STG). MEG offers a superior spatial resolution over EEG as it is unaffected by tissue boundaries, while keeping temporal precision (Dalal et al., 2008; Korvenoja et al., 2006), thus offering a potentially more sensitive measure to identify subtle MMN deficits. However, there are very few MEG-based studies looking at MMN sources at or before SZ onset. Shin et al. (2009) investigated individuals with clinical high risk for psychosis and found reduced MMN in right STG. Valt et al. (2022) reported reduced MMN sources in STG and bilateral transverse temporal sulcus and gyrus in FEP. Braeutigam et al. (2018) applied dynamic causal modeling in MEG data from 16 FE_{SZ} adolescents to find different inter-hemispheric connectivity patterns in FE_{SZ} and controls. On the other hand,

attempts to determine cortical areas involved in SZ MMN deficits have been restricted to anatomically rather than functionally defined areas (e.g. supratemporal plane, Heschl's gyrus (HG)), lacking the necessary precision to, for instance, distinguish between primary and secondary auditory areas. Human Connectome Project multimodal parcellation (HCP-MMP) pipelines (Glasser et al., 2013) overcome this restriction by using multimodal MRI data to delineate auditory cortex core and belt areas (Curtis et al., 2021).

In the present study, we aimed to localize distributed cortical MMN sources more effectively in FE_{SZ} by combining MEG inverse solutions with realistic individual MRI-based head models and by parcellating auditory cortical areas using HCP-MMP pipelines, all to determine possible MMN deficits more precisely in the early disease course. A better understanding of the locations affected early may help characterize the pathophysiology underlying impaired deviance detection in SZ and help to identify targets for further study and therapeutic interventions. Further, improved localization of the cortical activity underlying MMN may increase the sensitivity to the subtle pathology in early psychosis, critical for use as an endophenotype or biomarker of disease presence at or before the emergence of psychosis.

2 | METHOD

2.1 | Participants

A total of 32 healthy controls (C) and 35 first-episode psychosis (FEP) individuals were recruited from UPMC Western Psychiatric Hospital inpatient and outpatient services. Main analyses were performed on a subsample of 26 first-episode schizophrenia spectrum individuals (FE_{SZ}), and 26 matched controls (C), after removing eight individuals with diagnoses of affective disorders with psychotic features (bipolar disorder or major depression: FE_{Aff}) and one additional FE_{SZ} and six healthy controls for matching purposes (Table 1).

Among 27 FE_{SZ} individuals, 17 received diagnoses of schizophrenia (paranoid: $n = 8$; undifferentiated: $n = 8$; residual: $n = 1$), one of schizoaffective disorder, three of schizophreniform disorder, and six of psychotic disorder not otherwise specified (NOS). The rest of FEP individuals (8) received diagnoses of affective disorders (FE_{Aff}; bipolar: $n = 5$; major depressive: $n = 3$). All FEP individuals had less than 1 year of lifetime antipsychotic medication exposure and less than 1 year since either their first clinical contact (ER visit or hospitalization) or their first psychological or pharmacological treatment for psychosis (Table 2). Exclusion criteria for all participants were history of concussion or head injury with sequelae, history of alcohol or drug addiction in the last 5 years or neurological comorbidity. In addition, participants completed a pure-tone audiometry (1000–4000 Hz) before the experiment started, ensuring mean hearing thresholds below 30 dBnHL at each ear and less than 15 dB threshold differences between ears. All procedures were approved by the University of Pittsburgh IRB and in accordance with the WMA Declaration of Helsinki Ethical Principles for Medical Research Involving Human Subjects. All participants provided written informed consent and were paid for participation.

Groups were matched for age, gender, parental socioeconomic status (SES; measured with Hollingshead Scale, Hollingshead, 1975) and premorbid IQ as measured with the vocabulary subtest of the Wechsler Abbreviated Scale of Intelligence (WASI) (Table 2). The WASI vocabulary subtest is an IQ measure relatively resistant to psychosis and neurodegeneration (Bilder et al., 1988; Eberhard et al., 2003; Mohn-Haugen et al., 2022). Diagnoses from FEP individuals were based on the Structured Clinical Interview for DSM-IV (First et al., 2015), and their symptoms were rated using the Positive and Negative Syndrome Scale (PANSS; Kay et al., 1987). All tests were conducted by an expert clinical diagnostician.

Consistent with their illness, FEP individuals had significantly lower SES, WASI Matrix Reasoning subtest *t*-scores and current cognitive ability as assessed with the MATRICS Consensus Cognitive Battery (MCCB;

TABLE 1 Diagnostic assessments of patients in our sample.

First-episode psychosis (FEP $n = 35$)	
First-episode schizophrenia spectrum (FE_{SZ} $n = 27$[a])	**Affective disorders with psychotic features (FE_{Aff} $n = 8$)**
Schizophrenia—paranoid ($n = 8$)	Bipolar ($n = 5$)
Schizophrenia—undifferentiated ($n = 8$)	Major depression ($n = 3$)
Schizophrenia—residual ($n = 1$)	
Schizoaffective disorder ($n = 1$)	
Schizophreniform disorder ($n = 3$)	
Psychotic disorder not otherwise specified (NOS, $n = 6$)	

[a]One individual from this subgroup was discarded for matching purposes, resulting in a final $n = 26$.

TABLE 2 Demographic, neuropsychological and clinical data from 32 C versus 35 FEP (left panel) and from 26 C and 26 FE_{sz} (right panel). For both groups, mean (standard deviation) of age, parental socio-economic status (PSES), SES, WASI Vocabulary and Reasoning subtest *t* scores and MCCB composite scaled *t* scores are provided. For FEP only, PANSS total, positive and negative scores, duration in days from psychosis onset to scan (PSYC2SCAN) and from medication to scan (MED2SCAN) and chlorpromazine-equivalent dose (CPZmed) are provided. Independent-samples Student's *t*-test (degrees of freedom) and their associated *p* values are provided. *P* values below .05 are highlighted in bold. For gender only, Pearson chi-square values are provided.

	35 FEP vs. 32 C				**26 FE_{sz} vs. 26 C**			
	FEP	**C**	**$T_{(65)}/X^2$**	***p***	**FE_{sz}**	**C**	**$T_{(50)}/X^2$**	***p***
Age	22.7(3.7)	24.4(4.9)	1.57	.12	22.7(3.8)	24.7(5.0)	1.59	.11
Gender (M/F)	26/9	18/14	2.41	.12	20/6	15/11	2.18	.13
PSES	42.5(14.4)	47.1(9.7)	1.54	.12	40.4(13.2)	44.8(8.7)	1.39	.16
SES	29.9(11.3)	45.1(10)	5.54	**<.001**	30.8(11.8)	44.4(10.6)	4.36	**<.001**
WASI Vocab	49.6(7.8)	51.8(5.1)	1.35	.18	49.0(8.4)	51.1(5.1)	1.07	.29
WASI Reas	51.7(8.9)	59.0(5.6)	4.00	**<.001**	51.6(9.2)	58.8(6.2)	3.29	**.002**
MCCB-total	33.2(13.9)	51.9(8.0)	6.78	**<.001**	32.1(15.4)	51.1(8.0)	5.60	**<.001**
PANSS T	73.8(18.2)				75.7(16.6)			
PANSS P	18.7(5.9)				19.5(5.6)			
PANSS N	17.1(6.4)				17.5(6.5)			
PSYC2SCAN	75.2(87.7)				68.4(88.0)			
MED2SCAN	77.2(89.1)				66.4(89.2)			
CPZmed	253.7(148.9)				264.1(164.1)			

Nuechterlein et al., 2008). The majority of FEP individuals were medicated (only two FE_{sz} were not), but chlorpromazine-equivalent dose (CPZmed) did not correlate with any neuroimaging measure in any condition (*p* values > .4).

2.2 | Stimuli and procedure

The tone sequence consisted of an oddball paradigm with standard tones (1 kHz, 50 ms duration, 5 ms rise/fall, 80 dB), pitch deviants (1.2 kHz, 50 ms duration, 5 ms rise/fall, 80 dB) and duration deviants (1 kHz, 100 ms duration, 5 ms rise/fall, 80 dB), presented with a stimulus-onset asynchrony (SOA) of 330 ms (Figure 1). A total of 1600 tones were presented, including 1280 standards (80%), 160 pitch deviants (10%) and 160 duration deviants (10%). Deviants never followed another deviant, with a minimum of two standards intervening. All stimuli were created using Ace of Wav (Polyhedric Software) and delivered through ER-3A insert earphones (Etymotic Research, Inc., Elk Grove Village, IL, USA) using Presentation® software (Version 9.90). During the recordings, participants sat in the MEG/EEG scanner in a magnetically shielded room while passively listening to the tone sequence. They were instructed to watch a silent movie without subtitles and ignore the sounds.

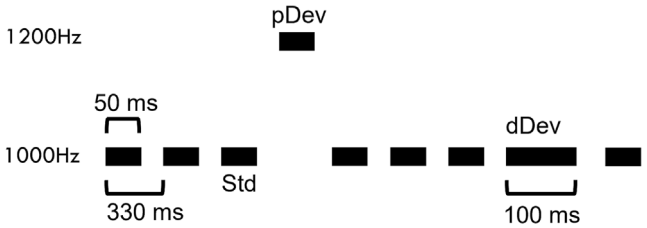

FIGURE 1 Example of the stimulation sequence. Oddball paradigm with standard (1 kHz, 50 ms length), pitch deviant (1.2 kHz, 50 ms length) and duration deviant (1 kHz, 100 ms length) tones. All tones were presented at 80 dB and with an SOA of 330 ms.

2.3 | MRI acquisition and processing

Structural and functional MRIs from each participant were obtained for use in MEG source solutions. T1-weighted (T1w) anatomical MR images were acquired using a Siemens 3-T MAGNETOM Prisma system with a multi-echo 3D MPRAGE sequence (relaxation time/echo time/inversion time = 2400/2.22/1000 ms, flip angle = 7°, field of view [FOV] = 256 × 240 mm, 0.8 mm isotropic voxel size, 208 slices, GRAPPA acceleration factor = 2). T2-weighted (T2w) T2-SPACE images were similarly obtained (relaxation time = 3200 ms, echo time = 563 ms, FOV = 256 × 240, 0.8 mm isotropic voxel size, 208 slices), along with a standard fieldmap for correcting readout

distortion in the T1w and T2w images. Finally, 10 min of eyes-open resting state BOLD fMRI data were obtained using a multiband pulse sequence (relaxation time = 800 ms, echo time = 37 ms, multiband factor = 8, flip angle = 52°, FOV = 208 × 208 mm, voxel size = mm^3, 72 slices).

HCP-MMP pipelines were then applied to process MRI data (see Glasser et al., 2013). A detailed summary of these procedures can be found in a recent report from our laboratory (Curtis et al., 2023). The main outcomes from this step were (1) individual's native-mesh cortical surface generated by extracting white and pial surfaces from native space images, refined using T2w data (Dale et al., 1999); and (2) HCP-MMP annotation files with parcellations mapped and sampled to individual's cortical surface. Both these outcomes were imported to Brainstorm software (Tadel et al., 2011) to be co-registered with MEG activity from source analysis. This allowed us to delineate precise functionally meaningful auditory cortical areas in individual's native MRI space, which would later be used to accurately label MEG source locations (see MEG source localization methods below). In addition, grey matter volumetric data were calculated from auditory cortical areas using the HCP-MMP atlas and FreeSurfer.

Structural data were missing or incomplete for three patients: In two cases, MRI data from a follow-up MRI scan 3 months after the baseline one were used instead. In the third case, only a T1 could be retrieved, and Brainstorm-DUNEuro MRI parcellation routine (Medani et al., 2021; Schrader et al., 2021) was used instead to delineate HCP-MMP annotation files. In all these cases, replacement structural data were only used for the purpose of MEG inverse solutions but discarded for grey matter volumes calculations.

2.4 | MEG acquisition and processing

Combined EEG and MEG acquisition was performed in a magnetically shielded room (Imedco AG, Hägendorf, Switzerland) using a low-impedance EEG cap (BrainCap MEG, Brain Vision, LLC, Morrisville, NC, USA) with 60 scalp electrode locations based on the 10-10 system and a 306 whole-head MEG system (Elekta Neuromag), consisting of 102 triplets (one magnetometer plus two planar gradiometers). Due to the poor quality of the EEG in 11 participants (five C and six FE) due to a circuit board failure, we analyzed MEG only. Data were recorded at a sampling rate of 1000 Hz, and online band-pass filtered from 0.1 to 330 Hz. Additional leads were placed in the left mastoid (online EEG reference), right mastoid, back of the neck (ground), below the left clavicle (ECG) and below the left eye (VEOG). Two bipolar electrodes were also placed on the outer canthi of both eyes (HEOG). Participant's head position relative to the MEG sensors was continuously monitored through the experiment by using a 3D digitizer (ISOTRAK; Polhemus, Inc., Colchester, VT) tracking the position of four head position indicator (HPI) coils placed on participant's head (relative to the nasion and preauricular points). Additional locations on participant's head and face, including nasion and left- and right-ear pre-auricular points, were tracked using the same digitizer to aid the coregistration of MRI and MEG data.

Electromagnetic noise originated outside of the MEG helmet was removed by using the temporal extension of the Signal Space Separation method (Taulu et al., 2004; Taulu & Simola, 2006), and motion effects on MEG sensor data were corrected using Neuromag MaxFilter software (Taulu & Simola, 2006). Data were high-pass filtered (0.5 Hz; 12 dB/oct) and visually inspected to remove sensors and segments of data containing excessive noise using EEGLAB Toolbox (Delorme & Makeig, 2004). Still on EEGLAB, eye blinks, horizontal eye movements and ECG components were isolated and removed from the data by using adaptive mixture independent component analysis (AMICA). Components were identified based on their topography and temporal dynamics, and only one component was removed for each artefact type.

Subsequent MEG data processing and source localization were conducted using Brainstorm software (Tadel et al., 2011). Continuous MEG data were low-pass filtered (20 Hz; 24 dB/oct), and epochs of −50 to 300 ms (baseline corrected) were extracted around the auditory stimulus. Epochs with MEG signal exceeding ±2.5 pT were discarded. The remaining epochs were averaged to isolate evoked responses to each condition. pMMN and dMMN were obtained by subtracting the standard average from each of the deviant averages.

2.5 | MEG source localization

The locations of possible dipole sources were constrained to the individual's native cortical surface, segmented during MRI processing (see Section 2.3). This cortical surface was then tessellated into an icosahedron mesh with 15,000 vertices per hemisphere, where each vertex constituted a potential dipole. The locations of the MEG sensor locations were coregistered with the structural images from each participant in two steps: (1) by aligning the three fiducial points digitized in the participant during MEG acquisition (nasion and left- and right-ear pre-auricular points) with their correspondent points manually marked in the MRI image and (2) by manually inspecting the

coregistration using the additional digitized points in participant's face and head and an MRI head surface generated with FreeSurfer as part of the HCP-MMP pipelines. The forward solution was modeled as overlapping spheres (one per sensor), and a noise covariance matrix was calculated from the baseline window (−50–0 ms) of all trials.

Cortical source activity was then calculated for the standard, pitch deviant and duration deviant averages using minimum norm estimation (Gramfort et al., 2014). Specifically, the forward solution and the noise covariance matrix were used to create a linear inverse operator using a loose orientation constraint of 0.4 (0 = fully orthogonal to cortex; 1 = no constraint) (Lin et al., 2006) and depth-weighting applied. The resulting current density values obtained at each of the 30,000 vertices of the cortical source space were then normalized using dynamic statistical parametric maps (dSPM) based on the variance in the pre-stimulus baseline. dSPM values from vertices within each HCP-MMP parcel (e.g. A1 or LBelt) were averaged and extracted from each subject for statistical comparisons. Concurrently, cortical source values were also morphed into a common space (MNI-ICBM152) with 10 mm smoothing to visualize source maps averaged across subjects.

2.6 | Statistical analysis

Repeated measures ANOVAs with a within-subjects (hemisphere) and a between-subjects factor (group) were performed separately for pMMN and dMMN source activity averaged over a 70–170 ms and a 110–210 ms time window, respectively. The selection of these time windows was based on MMN peaks at the butterfly plot grand-average waveforms (Figure 2). Independent-samples *t*-tests were computed for planned comparisons comparing groups in each hemisphere separately. Exploratory correlations of MMN cortical sources differing between groups with their structural MRI volumes, symptoms (total, negative and positive PANSS), cognition (WASI Vocabulary and Reasoning subtest *t* scores, MCCB composite scaled *t* scores), social functioning (global functioning: role, global functioning: social) and duration of illness (psychosis to scan) were computed using the Spearman correlation coefficient. All analyses were carried out using IBM SPSS Statistics (Version 26).

3 | RESULTS

3.1 | MEG sensor data

Pitch and duration MMN waveforms averaged across subjects from each group are provided in Figure 2 for each of the 102 magnetometers. Sizable MMN to pitch and duration deviants were observed in both groups. The overall morphology of the event-related field was as expected, with pMMN and dMMN peaking at approximately 110 and 160 ms, respectively, as in previous reports using the same experimental paradigm (Curtis et al., 2021; Murphy et al., 2020; Salisbury et al., 2020). The latency shift in dMMN is consistent with stimulus deviance arriving 50 ms after sound onset, the expected duration. These butterfly plots indicate the low pre-stimulus activity as well as the expected evoked response activity across the head.

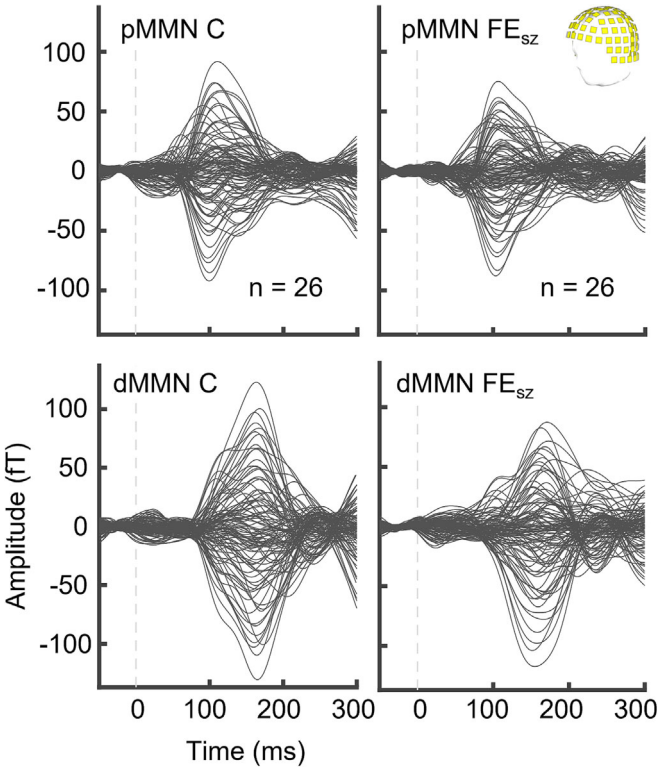

FIGURE 2 Pitch (top) and duration (bottom) MMN event-related fields averaged across C (left) and FE$_{sz}$ (right) participants for the 102 magnetometers. Sizable MMN to pitch and duration deviants were observed in both groups.

3.2 | MEG sources data

Results from MEG inverse solutions revealed pMMN and MMN sources were primarily located in bilateral auditory cortex (Figure 3) in both groups, with the strongest source activity observed in its sensory subdivisions (core, belt and parabelt areas, delineated as A1, MBelt, LBelt and PBelt HCP-MMP parcels in Figure 3). Mean MMN source activity for each auditory cortex parcel and hemisphere are provided in Table 3, separately for condition and group.

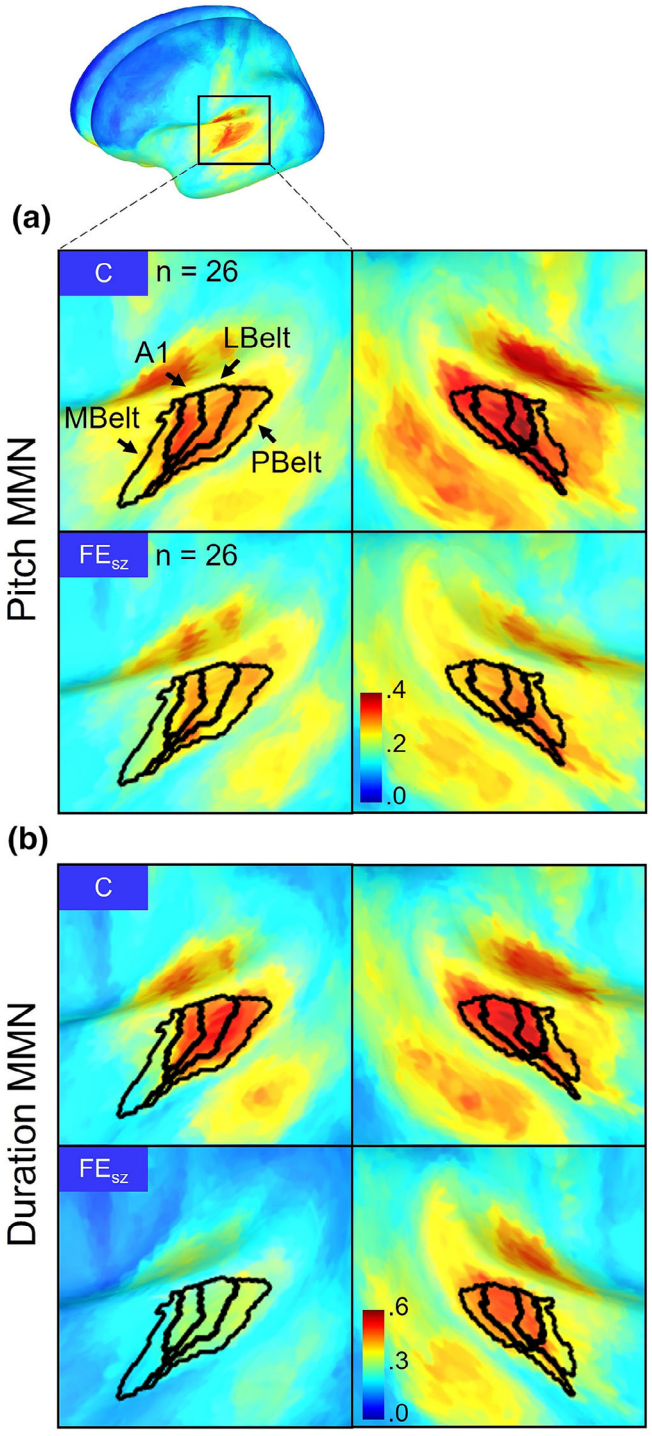

FIGURE 3 Cortical source maps of MMN response projected onto an MNI-ICBM152 brain template and averaged across subjects, separately for FE_{sz} and C groups. Pitch (a) and duration (b) MMN dSPM values were averaged across a time window of 70–170 ms and 110–210 ms, respectively. Left (left panels) and right (right panels) hemisphere activity is shown. The auditory cortex main subdivisions (A1, MBelt, LBelt, PBelt) as delineated by the Human Connectome Project multimodal parcellation (HCP-MMP) are displayed in the top left panel. MMN sources were primarily located at bilateral auditory cortex.

Rather than comparing source activity between groups over a broad auditory cortex area (e.g. HG, supratemporal cortex), we centered our statistical analyses in each auditory cortex parcel separately (A1, MBelt, LBelt and PBelt) as more precise and functionally meaningful cortical areas. Specifically, we focused on A1 as the parcel with the largest source activity values in our solution. Source waveforms for A1 are displayed in Figure 4a. Clear

TABLE 3 MMN cortical source activity averaged across subjects. Averaged dSPM source values (mean ± SD) within each auditory cortex parcel separated by condition (pMMN: 70–170 ms; dMMN: 110–210 ms) and hemisphere (left and right).

	FE_{sz} ($n = 26$)		C ($n = 26$)	
	pMMN	**dMMN**	**pMMN**	**dMMN**
Left A1	0.28 ± 0.20	0.30 ± 0.15	0.32 ± 0.16	0.47 ± 0.32
Right A1	0.27 ± 0.15	0.46 ± 0.33	0.33 ± 0.19	0.51 ± 0.32
Left MBelt	0.20 ± 0.10	0.22 ± 0.10	0.26 ± 0.16	0.29 ± 0.18
Right MBelt	0.28 ± 0.18	0.38 ± 0.222	0.32 ± 0.16	0.44 ± 0.18
Left LBelt	0.26 ± 0.16	0.28 ± 0.13	0.27 ± 0.12	0.41 ± 0.26
Right LBelt	0.28 ± 0.18	0.47 ± 0.34	0.34 ± 0.20	0.51 ± 0.31
Left PBelt	0.28 ± 0.18	0.30 ± 0.14	0.28 ± 0.18	0.43 ± 0.26
Right PBelt	0.28 ± 0.17	0.28 ± 0.17	0.32 ± 0.17	0.32 ± 0.17

MMN peaks were identified for both pitch and duration at the expected latencies and in both hemispheres. Mean MMN values from each participant were extracted from the highlighted time windows and are displayed in Figure 4b. To account for a non-normal distribution of source activity, a log10 transformation was applied to source data from all conditions and groups (hence the different scales in Figure 4a,b). The distributions with the original dSPM values can be found in Figure S1.

In pMMN, groups did not differ in A1 source activity when including both hemispheres in the model, although differences approached statistical significance ($F_{(1,50)} = 3.31$; $p = .07$; $\eta_p^2 = .06$). In light of the observed associations in FEP between scalp MMN and left auditory cortex grey matter volumes (Curtis et al., 2023; Salisbury et al., 2007, 2020), we compared left and right A1 source values between groups separately. Neither left ($t_{(50)} = 1.20$; $p = .23$; $d = .33$), nor right ($t_{(50)} = 1.57$; $p = .12$; $d = .43$) A1 pMMN values differed between groups.

In dMMN, A1 activity was reduced in FE_{sz} ($F_{(1,50)} = 4.11$; $p = .04$; $\eta_p^2 = .07$), independent of hemisphere (hemisphere by group interaction: $F_{(1,50)} = .82$; $p = .36$; $\eta_p^2 = .01$). As previously stated, hypothesis-driven group comparisons were computed separately for each hemisphere. Those comparisons showed that left ($t_{(56)} = 2.23$; $p = .03$; $d = .61$) but not right ($t_{(56)} = 1.02$; $p = .31$; $d = .28$) A1 activity was reduced in the FE_{sz} group.

Significant MMN reductions in FE_{sz} were not observed in any of the other auditory cortex parcels where source activity was identified, neither for pMMN (MBelt: $F_{(1,50)} = 2.31$; $p = .13$; $\eta_p^2 = .04$; LBelt: $F_{(1,50)} = 2.44$; $p = .12$; $\eta_p^2 = .04$; PBelt: $F_{(1,50)} = 2.45$; $p = .12$; $\eta_p^2 = .04$) nor for dMMN (MBelt: $F_{(1,50)} = 3.39$; $p = .07$; $\eta_p^2 = .06$; LBelt: $F_{(1,50)} = 3.43$; $p = .07$; $\eta_p^2 = .06$; PBelt: $F_{(1,50)} = 3.48$; $p = .06$; $\eta_p^2 = .06$), although with group differences approached statistical significance for the latter.

3.3 | Differences between FE_{sz} and FE_{Aff}

To assess the specificity of MMN impairment as a phenotype of schizophrenia, we compared the distributions of MMN source activity in A1 among healthy controls, FE_{Aff} and FE_{sz} (Figure 5). No ANOVAs were computed between the two FE groups or between the C and the FE_{Aff}, due to the reduced number of affective psychosis individuals and the impossibility to match subgroups by age, gender, WASI Vocab and PSES. Despite that, in both hemispheres and for the two deviant types, we observed almost identical group means for affective psychosis individuals and controls, with only the FE_{sz} group means being smaller. Effect sizes when comparing C and FE_{Aff} group means were small for pMMN (left: $d = .13$; right: $d = .29$) and negligible for dMMN (left: $d = .01$; right: $d = .11$). The same comparison between FE_{Aff} and FE_{sz} groups yielded overall much larger effect sizes for both pMMN (left: $d = .57$; right: $d = .84$) and dMMN (left: $d = .76$; right: $d = .27$). We speculate from this that individuals with affective psychosis may preserve healthy MMN responses at their first-episode phase.

As a separate analysis, we compared MMN source values in A1 within our largest samples including affective psychosis first-episode participants (27 FE_{sz} + 8 FE_{Aff} = 35 FEP vs. 32 matched controls). Results replicated those found in the smaller samples. A1 pMMN reduction in FEP group only approached statistical significance ($F_{(1,65)} = 3.50$; $p = .06$; $\eta_p^2 = .05$), and comparisons at each hemisphere for this condition revealed no specific MMN reduction in either left-hemisphere ($t_{(65)} = 1.27$; $p = .20$; $d = .31$) or right-hemisphere ($t_{(65)} = 1.66$; $p = .09$; $d = .40$) A1. A1 dMMN was overall reduced in FEP ($F_{(1,65)} = 4.87$; $p = .03$; $\eta_p^2 = .07$). When testing each hemisphere individually, only left A1 showed a diminished MMN signal in FEP (left: $t_{(65)} = 2.19$; $p = .03$; $d = .53$. Right $t_{(65)} = 1.34$; $p = .18$; $d = .32$). Given the apparent

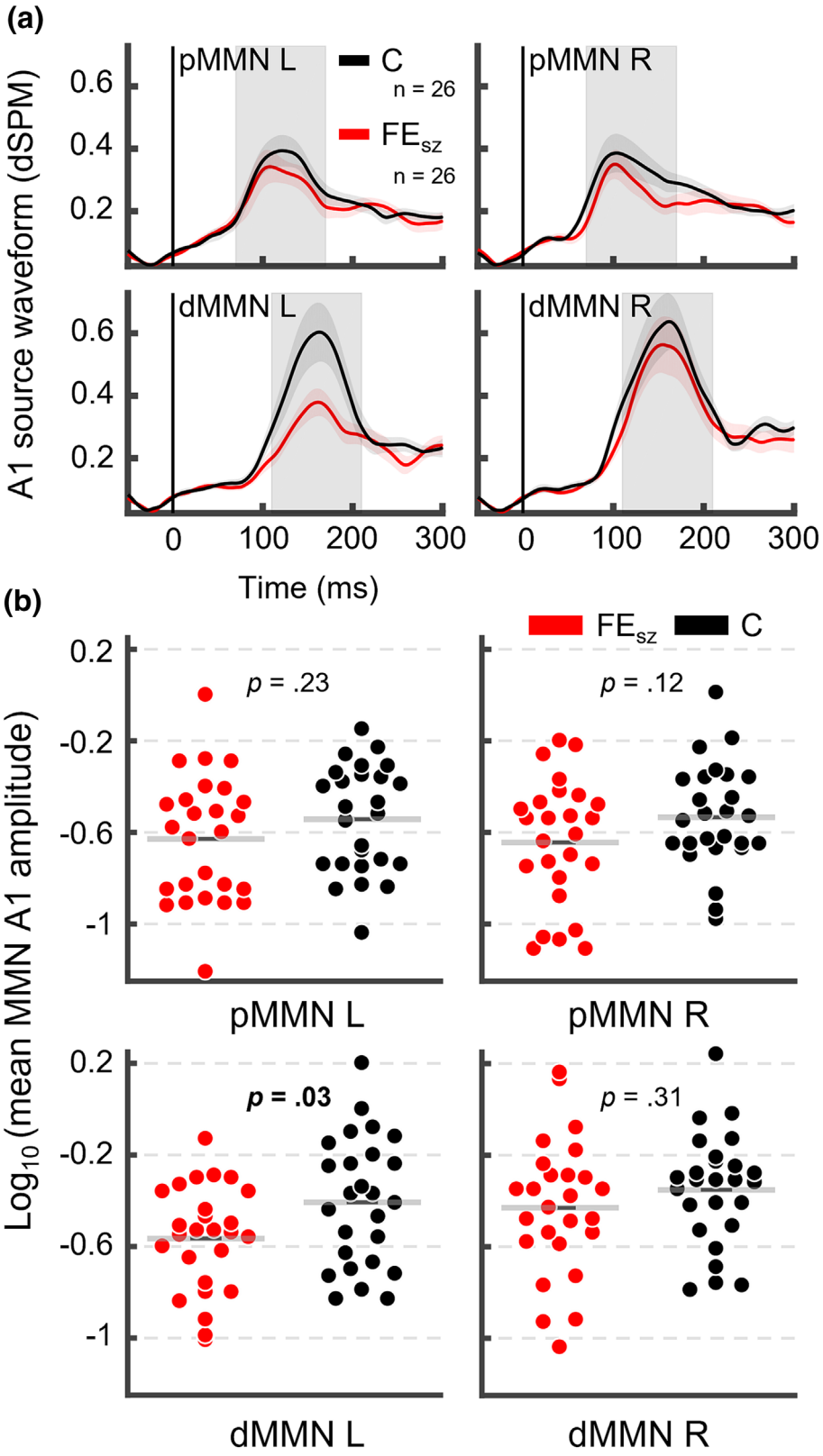

FIGURE 4 (a) MMN source waveforms (dSPM values) from HCP-MMP-delineated A1 averaged across subjects, separately for FE_{sz} (red) and C (black) groups. Shaded areas around the waveform line indicate the standard error of the mean (SEM). Areas in grey highlight the time windows from which MMN averages were computed (70–170 for pMMN; 110–210 for dMMN). (b) Scatter plots of MMN mean amplitudes in A1 parcel. A log10 transformation of original dSPM values was performed due to some outlier values (see Figure S1). For each hemisphere and condition, *p* values from independent-samples *t*-tests comparing groups are displayed (*p* values below .05 are highlighted). Only left A1 dMMN values were significantly reduced in FE_{sz}.

differences observed in A1 dMMN between FE_{sz} and FE_{Aff}, dMMN reduction in FEP group may be driven primarily by FE_{sz} and hold due to increased power with larger *n*'s.

3.4 | MRI volumetric data

There were no auditory cortex parcels (A1, MBelt, LBelt and PBelt) where grey matter volumes significantly

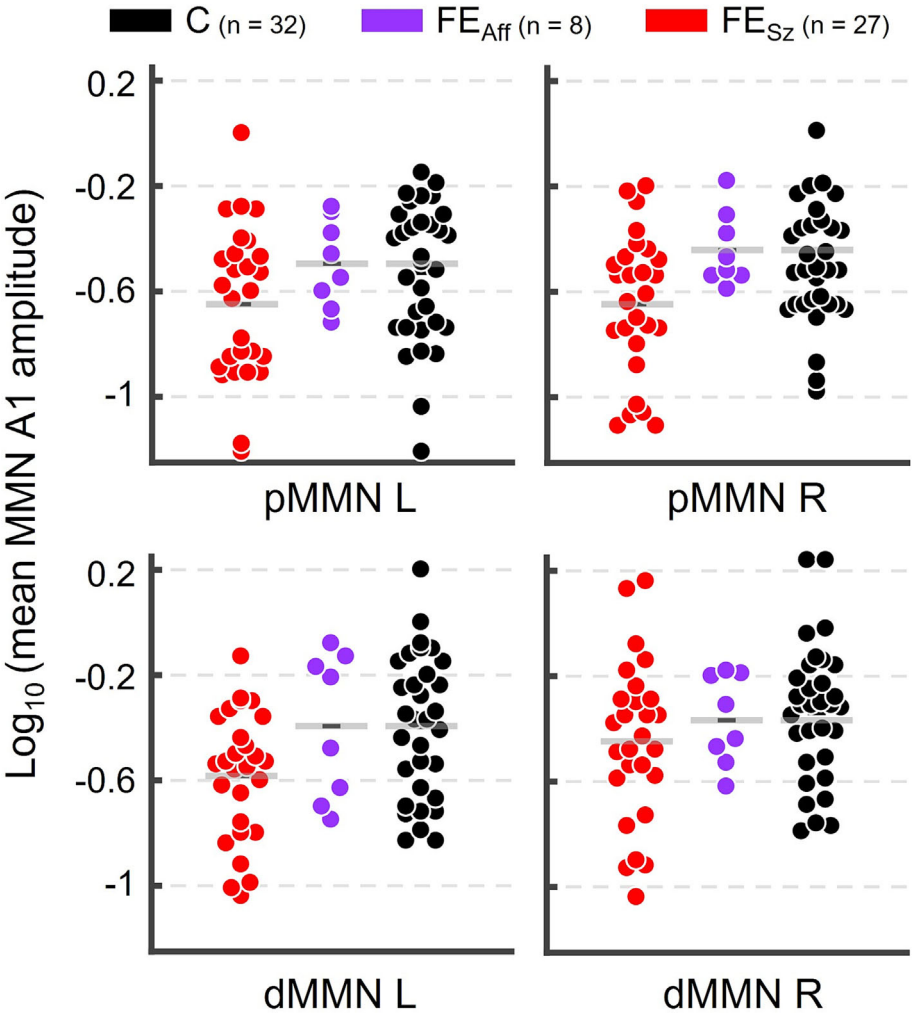

FIGURE 5 Scatter plots of MMN averaged source activity in A1 parcel for our largest control group ($n = 32$) and for FE_{sz} ($n = 27$) and FE_{Aff} ($n = 8$) groups separately. A log10 transformation of original dSPM values was performed to reduce variation caused by some outliers. FE_{Aff} source activity values are closer to those of controls than FE_{sz}.

differed between groups (p's > .05) when correcting for multiple comparisons (Benjamini–Hochberg's FDR correction), either with FE_{sz} or with FEP groups. Grey matter volume averages and detailed results of the statistical comparisons can be found in Tables S1–S4.

3.5 | Exploratory correlations with MRI volumes and clinical data

There were no significant correlations of MEG dMMN and grey matter volumes in A1 (p's > 0.05), as shown in Table 4. Likewise, A1 dMMN source activity did not correlate with most clinical measures, with the exception that dMMN activity in right A1 was negatively correlated with duration of illness (number of days from the first psychosis-related hospitalization/ER visit/treatment to scan), both in FE_{sz} and FEP groups (Table 4). That is, the longer the duration of illness, the more impaired right A1 MMN was (smaller source values in a log10 scale). However, such correlation did not survive Benjamini–Hochberg's FDR correction.

4 | DISCUSSION

MEG sources of pMMN and dMMN were localized primarily in the auditory cortex core (A1), and in lateral belt and parabelt areas, with no differences in location between groups or conditions. Duration but not pitch MMN in left A1 was reduced in FE_{sz} and FEP groups relative to matched controls, with a larger effect size ($d = .61$) than those reported in scalp-MMN meta-analyses ($d = .47$; Haigh et al., 2017). dMMN group differences in belt areas only approached statistical significance. When separating FE_{sz} and FE_{Aff} psychosis groups, A1 dMMN from affective psychosis individuals appeared unaffected relative to controls.

MMN source locations in the present study were consistent with reports of MMN generators in healthy individuals, where primary sources were found in bilateral primary and secondary auditory cortices using EEG and MEG inverse solutions (Alho, 1995; Giard et al., 1990; Hari et al., 1992; Rinne et al., 2000), fMRI (Molholm et al., 2005) and intracranial recordings (Kropotov et al., 1995; Rosburg et al., 2005). We failed to replicate

TABLE 4 Spearman's rho correlations (ρ) of dMMN in left and right A1 (log transformed) with clinical and structural data: PANSS total, positive and negative scores, duration in days from psychosis onset to scan (PSYC2SCAN) and from medication to scan (MED2SCAN), chlorpromazine-equivalent dose (CPZmed) and HCP-MMP parcellated A1 volumes. Associated *p* values are provided, uncorrected for multiple comparisons. *P* values below 0.05 are highlighted in bold. No *p* value survived Benjamini–Hochberg's FDR correction.

	dMMN FEP ($n = 35$)				dMMN FE_{sz} ($n = 26$)			
	Left		Right		Left		Right	
	ρ	*p*	ρ	*p*	ρ	*p*	ρ	*p*
PANSS T	−.160	.360	.096	.582	.080	.699	.419	**.033**
PANSS P	−.166	.339	−.024	.890	.087	.673	.156	.447
PANSS N	−.178	.307	−.005	.977	−.045	.828	.209	.306
PSYC2SCAN	−.110	.528	−.408	**.015**	−.233	.253	−.447	**.022**
MED2SCAN[a]	.117	.517	−.279	.116	−.065	.762	−.323	.124
CPZmed[a]	−.051	.780	.068	.707	−.011	.958	.066	.761
Volume A1 L[b]	−.084	.649	.099	.590	.018	.933	.033	.878
Volume A1 R[b]	−.020	.914	.155	.396	.111	.604	.044	.838

[a]Two FEsz patients were not medicated ($n = 33$ FEP and 24 FEsz).
[b]No structural data available for two FEsz and one FEAff patients ($n = 32$ FEP and 24 FEsz).

feature-dependent generators as observed by Molholm et al. (2005), albeit the different nature of the measure taken (inferred current vs blood flow) could influence the results. Some reports also indicate frontal generators (Rinne et al., 2000), specifically in the inferior frontal gyri (IFG) (Alain et al., 1998; Park et al., 2002), which we did not observe. This could be due to the MEG being less sensitive to both dipoles radial to the surface of the head (Baillet, 2017; Hillebrand & Barnes, 2002), thus capturing less activity from frontal gyri, and to anterior sources (Marinkovic et al., 2004).

Within auditory cortex, our results suggested A1 was the strongest MMN generator and the one impaired in FE_{sz}, although with strong contributions from lateral belt and parabelt as well. These fit well with findings from animal literature locating main cortical generators of MMN-like responses in A1, both in monkeys (Fishman & Steinschneider, 2012; Javit et al., 1994; Lakatos et al., 2020) and in mice (Chen et al., 2015). In rats, Shiramatsu et al. (2013) found sources in both the core and belt regions of auditory cortex. In animal models of SZ measuring MMN, subanesthetic administration of NMDA antagonists reduced MMN amplitude in A1 (Javitt et al., 1996). However, it is also possible that our parcellation resolution exceeds source localization resolution. Still, we speculate this is not the case as we saw discrete puncta in the different auditory sensory cortex parcels (see also Curtis et al., 2023).

MMN to duration deviants was the more greatly affected in FE. In line with previous reports (Magno et al., 2008; Salisbury et al., 2002; Valkonen-Korhonen et al., 2003), we did not find significant reductions in pMMN in FE, even at the source level. With the effect sizes found for pMMN ($d = .03$ and $d = .04$ for left and right hemisphere, respectively), we would need approximately 200 individuals per group to observe FE_{sz} pMMN reduction at alpha = 0.05. While both pMMN and dMMN are severely reduced in long-term SZ (Salisbury et al., 2002; Shelley et al., 1991), dMMN appears to be affected earlier, and with effect sizes about 40% larger throughout the course of the disease (Umbricht & Krljes, 2005). Michie (2001) discussed several hypotheses potentially explaining this phenomenon. First, based on (Rammsayer, 1990) findings of impaired temporal discrimination in SZ, it was suggested that SZ patients have specific difficulties processing the temporal features of auditory stimuli, thus impairing their ability to detect deviance in the temporal dimension. To that regard, Todd et al. (2000) observed dMMN impairments in SZ patients despite using duration increments in the deviant stimuli well above their duration discrimination threshold (50 vs. 100 ms, also used in the present study), thus suggesting temporal discrimination may not account for dMMN deficits (but see Todd et al., 2003). Second, reduced dMMN may be related to an abnormal window of temporal integration (Michie, 2001). Longer auditory stimuli are also perceived as louder due to the temporal integration of acoustic energy, particularly over the first 200 ms of a sound (window of temporal integration; Näätänen et al., 1992). Thus, a longer sound could be conceived as a deviant triggering the auditory network of deviance detection to a greater degree than a single (pitch) deviant. Reduced dMMN in SZ only occurs with short stimuli falling under that time window, supporting

an abnormal window of temporal integration in the disease (Michie, 2001).

The differential impairment of pMMN and dMMN in SZ could also be related to morphologic abnormalities affecting their respective generators differently. A recent study from our laboratory (Curtis et al., 2021) found EEG pMMN and dMMN in FEP were related to grey matter volume loss in slightly different areas. While the lack of correlations between MMN sources and structural volumes in the present study cannot support that hypothesis, we did observe dMMN deficits were hemispheric-specific. Conversely, a common more generalized cortical affectation in the disease, such as NMDA receptor hypofunction (Olney et al., 1999), could be more damaging for areas involved in temporal discrimination, such as the prefrontal cortex (Gooch et al., 2011; Merchant et al., 2013), thus affecting selectively the mechanisms responsible for the detection of duration deviants. Related to the last hypothesis, the processing of stimulus duration could also rely on more complex mechanisms requiring of additional neuronal resources as compared to pitch. The tonotopic organization of the cortex is also present in subcortical structures of the auditory pathway such as the inferior colliculus (Ress & Chandrasekaran, 2013) or the thalamus (Yvert et al., 2002), which are involved in the processing of stimulus pitch (Krishnan & Gandour, 2009). Thus, the detection of stimulus pitch could be more resilient to brain damage, while the processing of stimulus duration may be more sensitive to the yet subtle structural and functional deficits in the auditory brain during the early phase of the disease. The prominence of dMMN impairments in the present study also goes along with results of reduced theta inter-trial phase coherence specifically for duration deviants, both in early (Hua et al., 2023) and chronic SZ (Hochberger et al., 2019, 2020; Lee et al., 2017), and supports the hypothesis that MMN deficits in SZ reflect reduced theta-frequency activity (Javitt et al., 2000).

We found a dMMN reduction in patients that was localized in the left hemisphere. These results fit with previous findings from our laboratory where deficits in scalp dMMN in FEP were associated with reductions of grey matter volumes in the left auditory cortex (Curtis et al., 2021; Salisbury et al., 2020). Moreover, they are in line with reports of left temporal lobe structural abnormalities in FE (Hirayasu et al., 1998) and chronic schizophrenia (Kawasaki et al., 2008; Youn et al., 2003), specifically in areas involving MMN generation such as left HG (Kasai et al., 2003). Our results also relate to reports of reduced hemispheric volume asymmetry (left > right) in SZ (Smiley et al., 2009), specifically in A1 (Smiley et al., 2013). The auditory processing of sound duration in the left auditory cortex could thus be impaired as compared to the relatively healthy right counterpart due to the structural dysfunction of its cortical generators. Notably, the left temporal lobe appears to be specialized in the analysis of the timing and sequential properties of the auditory scene (Zatorre et al., 2002; Zatorre & Belin, 2001), which would explain why duration but not pitch MMN is affected. Despite the causes behind the exacerbated left vs. right structural abnormalities in SZ are outside the scope of the present study, we speculate that the different cytoarchitectonic organization of left and right auditory cortex (Harrison et al., 2010) may result in a differential sensitivity to the underlying pathophysiology and link with language-related symptoms such as auditory hallucinations and impaired verbal cognition (Heidrich & Strik, 1997). On the other hand, our results contrast with the few other EEG dipole-fitting (Oades et al., 2006; Randau et al., 2019) and MEG source-localization (Valt et al., 2022) studies in FE that found right (Randau et al., 2019) or bilateral dMMN reductions, suggesting further research is necessary to account for the variability of the source-reconstruction techniques applied in different studies.

The effect size of left A1 dMMN reduction in FE_{SZ} found in our sample ($d = .61$) was larger than those reported in meta-analyses for its scalp-recorded counterpart ($d = .47$; Haigh et al., 2017) and may thus be more useful to distinguish patients from controls at the group level. However, such effect size may still be insufficient to consider source-solved dMMN of clinical utility as a diagnostic biomarker, as for most FE_{SZ} individuals MMN amplitude overlapped with that of controls. While MEG source-solved MMN may still not be a good biomarker of SZ presence, it may be more sensitive than scalp MMN to the underlying neural mechanisms altered during the pathogenesis of SZ, particularly in the left hemisphere. Moreover, A1 dMMN impairment may be a specific phenotype of psychosis in SZ, as discussed below.

In separate exploratory analyses to assess the selectivity of MMN source activity as a biomarker or phenotype for FE_{SZ}, we looked at affective psychosis individuals (FE_{Aff}) separately in comparison to our controls and found that their pMMN and dMMN appeared to be unaffected, with distributions remarkably close to that of C and different than FE_{SZ}. Given the moderate-to-large effect size of MMN reduction in FE_{SZ} relative to FE_{Aff} (pMMN left: $d = .57$; right: $d = .84$; dMMN left: $d = .76$; right: $d = .27$), and despite the limitations of an underpowered sample ($n = 8$), we speculate group differences are present at the population level, suggesting MMN specificity of SZ phenotype. Our results, albeit underpowered, go along previous reports of MEG MMN in

adolescents with bipolar disorder (BD) with psychotic features in relation to controls and adolescents with SZ. A previous study with first-hospitalized SZ and BD individuals with psychosis showed larger MMN deficits longitudinally in SZ but not BD, and associated MMN amplitude with left HG volume only in SZ (Salisbury et al., 2007). Smaller grey matter volumes in HG of SZ but not BD were also found by Kasai et al. (2003). Conversely, other studies comparing FE_{sz} and affective-spectrum disorder have found similar MMN reductions (Kaur et al., 2011; Valt et al., 2022). Future studies tracking MMN deficits in FE_{sz} and FE_{Aff} longitudinally and with larger samples should resolve the specificity of the deficit.

5 | CONCLUSIONS

The present study is the first to source-localize pMMN and dMMN in first-episode schizophrenia combining MEG, realistic head models based on MRI anatomy and HCP-MMP pipelines to precisely delineate auditory cortical areas. MEG source analysis indicated a deficit in left A1 dMMN activity in FE_{sz} that appeared to be preserved in individuals with affective psychosis. Auditory cortex belt areas appeared less affected. This deficit may be masked in scalp-recorded EEG studies due to tissue boundaries. FE_{sz} may be associated with a selective left hemisphere MMN deficit centered in auditory cortex core, consistent with selective grey matter pathology of left auditory cortex proximal to psychosis onset. Finally, MEG source-solved MMN may not be of clinical utility as a diagnostic biomarker, but serves as a window to explore the neural mechanisms implicated in the disease onset. The present study had several limitations. Namely, (1) the modest sample size, particularly in the FE_{Aff} group, (2) the insensitivity of MEG to frontal sources, limiting our measure of IFG MMN generators, and (3) the lack of good EEG for most subjects, which would allow us to properly compare MEG source vs. scalp EEG sensitivity to MMN deficits in the same subjects.

AUTHOR CONTRIBUTIONS

Conceptualization: Fran López-Caballero, Brian A. Coffman, Dean F. Salisbury. *Methodology*: Fran López-Caballero, Brian A. Coffman, Dean F. Salisbury. *Investigation*: Fran López-Caballero, Brian A. Coffman. *Formal analysis*: Fran López-Caballero, Brian A. Coffman, Mark Curtis. *Writing*: Fran López-Caballero, Dean F. Salisbury. *Funding acquisition*: Dean F. Salisbury. *Resources*: Dean F. Salisbury. *Supervision*: Dean F. Salisbury.

ACKNOWLEDGEMENTS

This research was supported by funding from the National Institutes of Health (R01 MH108568 and MH113533). We thank Dylan Seebold, Vanessa Fishel, Natasha Torrence, Yiming Wang and Rebekah Farris for their assistance in data collection.

CONFLICT OF INTEREST STATEMENT

The authors declare that the research was conducted in the absence of any commercial or financial relationships that could be construed as a potential conflict of interest.

PEER REVIEW

The peer review history for this article is available at https://www.webofscience.com/api/gateway/wos/peer-review/10.1111/ejn.16107.

DATA AVAILABILITY STATEMENT

The MEG and MRI data that support the findings of this study will be available from a data repository (OpenNeuro) after its publication without an end date.

ORCID

Fran López-Caballero https://orcid.org/0000-0001-9194-2199
Dean F. Salisbury https://orcid.org/0000-0002-8533-0599

REFERENCES

Alain, C., Woods, D. L., & Knight, R. T. (1998). A distributed cortical network for auditory sensory memory in humans. *Brain Research*, *812*(1–2), 23–37. https://doi.org/10.1016/S0006-8993(98)00851-8

Alho, K. (1995). Cerebral generators of mismatch negativity (MMN) and its magnetic counterpart (MMNM) elicited by sound changes. *Ear and Hearing*, *16*(1), 38–51. https://doi.org/10.1097/00003446-199502000-00004

Alho, K., Woods, D. L., & Algazi, A. (1994). Processing of auditory stimuli during auditory and visual attention as revealed by event-related potentials. *Psychophysiology*, *31*(5), 469–479. https://doi.org/10.1111/j.1469-8986.1994.tb01050.x

Atkinson, R. J., Michie, P. T., & Schall, U. (2012). Duration mismatch negativity and P3a in first-episode psychosis and individuals at ultra-high risk of psychosis. *Biological Psychiatry*, *71*(2), 98–104. https://doi.org/10.1016/j.biopsych.2011.08.023

Baillet, S. (2017). Magnetoencephalography for brain electrophysiology and imaging. *Nature Neuroscience*, *20*(3), 327–339. https://doi.org/10.1038/nn.4504

Bilder, R. M., Degreef, G., Mukherjee, S., Pandurangi, A. K., Rieder, R. O., & Sackeim, H. A. (1988). Neuropsychological deterioration and CT scan findings in chronic schizophrenia. *Schizophrenia Research*, *1*(1), 37–45. https://doi.org/10.1016/0920-9964(88)90038-2

Braeutigam, S., Dima, D., Frangou, S., & James, A. (2018). Dissociable auditory mismatch response and connectivity patterns in

adolescents with schizophrenia and adolescents with bipolar disorder with psychosis: A magnetoencephalography study. *Schizophrenia Research*, *193*, 313–318. https://doi.org/10.1016/j.schres.2017.07.048

Chen, I. W., Helmchen, F., & Lütcke, H. (2015). Specific early and late oddball-evoked responses in excitatory and inhibitory neurons of mouse auditory cortex. *Journal of Neuroscience*, *35*(36), 12560–12573. https://doi.org/10.1523/JNEUROSCI.2240-15.2015

Cropley, V. L., Klauser, P., Lenroot, R. K., Bruggemann, J., Sundram, S., Bousman, C., Pereira, A., di Biase, M. A., Weickert, T. W., Weickert, C. S., Pantelis, C., & Zalesky, A. (2017). Accelerated gray and white matter deterioration with age in schizophrenia. *American Journal of Psychiatry*, *174*(3), 286–295. https://doi.org/10.1176/appi.ajp.2016.16050610

Curtis, M. T., Coffman, B. A., & Salisbury, D. F. (2021). Pitch and duration mismatch negativity are associated with distinct auditory cortex and inferior frontal cortex volumes in the first-episode schizophrenia spectrum. *Schizophrenia Bulletin Open*, *2*(1), sgab005. https://doi.org/10.1093/schizbullopen/sgab005

Curtis, M. T., Ren, X., Coffman, B. A., & Salisbury, D. F. (2023). Attentional M100 gain modulation localizes to auditory sensory cortex and is deficient in first-episode psychosis. *Human Brain Mapping*, *44*(1), 218–228. https://doi.org/10.1002/hbm.26067

Dalal, S. S., Guggisberg, A. G., Edwards, E., Sekihara, K., Findlay, A. M., Canolty, R. T., Berger, M. S., Knight, R. T., Barbaro, N. M., Kirsch, H. E., & Nagarajan, S. S. (2008). Five-dimensional neuroimaging: Localization of the time-frequency dynamics of cortical activity. *NeuroImage*, *40*(4), 1686–1700. https://doi.org/10.1016/j.neuroimage.2008.01.023

Dale, A. M., Fischl, B., & Sereno, M. I. (1999). Cortical surface-based analysis: I. segmentation and surface reconstruction. *NeuroImage*, *9*(2), 179–194. https://doi.org/10.1006/nimg.1998.0395

Delorme, A., & Makeig, S. (2004). EEGLAB: An open source toolbox for analysis of single-trial EEG dynamics including independent component analysis. *Journal of Neuroscience Methods.*, *134*, 9–21. https://doi.org/10.1016/j.jneumeth.2003.10.009

Devrim-Üçok, M., Keskin-Ergen, H. Y., & Üçok, A. (2008). Mismatch negativity at acute and post-acute phases of first-episode schizophrenia. *European Archives of Psychiatry and Clinical Neuroscience*, *258*(3), 179–185. https://doi.org/10.1007/s00406-007-0772-9

Eberhard, J., Riley, F., & Levander, S. (2003). Premorbid IQ and schizophrenia: Increasing cognitive reduction by episodes. *European Archives of Psychiatry and Clinical Neuroscience*, *253*(2), 84–88. https://doi.org/10.1007/s00406-003-0412-y

Erickson, M. A., Albrecht, M., Ruffle, A., Fleming, L., Corlett, P., & Gold, J. (2017). No association between symptom severity and MMN impairment in schizophrenia: A meta-analytic approach. *Schizophrenia Research: Cognition*, *9*, 13–17. https://doi.org/10.1016/j.scog.2017.05.002

Erickson, M. A., Ruffle, A., & Gold, J. M. (2016). A meta-analysis of mismatch negativity in schizophrenia: From clinical risk to disease specificity and progression. *Biological Psychiatry*, *79*(12), 980–987. https://doi.org/10.1016/j.biopsych.2015.08.025

First, M. B., Williams, J. B. W., Karg, R. S., & Spitzer, R. (2015). Structured clinical interview for DSM-5—Research version (SCID-5 for DSM-5, research version; SCID-5-RV). In *The encyclopedia of clinical psychology* (pp. 1–6). John Wiley & Sons. https://doi.org/10.1002/9781118625392.wbecp351

Fishman, Y. I., & Steinschneider, M. (2012). Searching for the mismatch negativity in primary auditory cortex of the awake monkey: Deviance detection or stimulus specific adaptation? *Journal of Neuroscience*, *32*(45), 15747–15758. https://doi.org/10.1523/JNEUROSCI.2835-12.2012

Giard, M. -H., Perrin, F., Pernier, J., & Bouchet, P. (1990). Brain generators implicated in the processing of auditory stimulus deviance: A topographic event-related potential study. *Psychophysiology*, *27*(6), 627–640. https://doi.org/10.1111/j.1469-8986.1990.tb03184.x

Glasser, M. F., Sotiropoulos, S. N., Wilson, J. A., Coalson, T. S., Fischl, B., Andersson, J. L., Xu, J., Jbabdi, S., Webster, M., Polimeni, J. R., van Essen, D. C., & Jenkinson, M. (2013). The minimal preprocessing pipelines for the human connectome project. *NeuroImage*, *80*, 105–124. https://doi.org/10.1016/j.neuroimage.2013.04.127

Gooch, C. M., Wiener, M., Cris Hamilton, A., & Branch Coslett, H. (2011). Temporal discrimination of sub- and suprasecond time intervals: A voxel-based lesion mapping analysis. *Frontiers in Integrative Neuroscience*, *5*, 59. https://doi.org/10.3389/fnint.2011.00059

Gramfort, A., Luessi, M., Larson, E., Engemann, D. A., Strohmeier, D., Brodbeck, C., Parkkonen, L., & Hämäläinen, M. S. (2014). MNE software for processing MEG and EEG data. *NeuroImage*, *86*, 446–460. https://doi.org/10.1016/j.neuroimage.2013.10.027

Haigh, S. M., Coffman, B. A., & Salisbury, D. F. (2017). Mismatch negativity in First-episode schizophrenia: A meta-analysis. *Clinical EEG & Neuroscience: Official Journal of the EEG & Clinical Neuroscience Society (ENCS)*, *48*, 3–10. https://doi.org/10.1177/1550059416645980

Hari, R., Rif, J., Tiihonen, J., & Sams, M. (1992). Neuromagnetic mismatch fields to single and paired tones. *Electroencephalography and Clinical Neurophysiology*, *82*(2), 152–154. https://doi.org/10.1016/0013-4694(92)90159-F

Harrison, P. J., Lewis, D. A., & Kleinman, J. E. (2010). Neuropathology of schizophrenia. In *Schizophrenia* (pp. 372–392). Wiley Blackwell.

Heidrich, A., & Strik, W. K. (1997). Auditory P300 topography and neuropsychological test performance: Evidence for left hemispheric dysfunction in schizophrenia. *Biological Psychiatry*, *41*(3), 327–335. https://doi.org/10.1016/S0006-3223(96)00030-3

Hermens, D. F., Ward, P. B., Hodge, M. A. R., Kaur, M., Naismith, S. L., & Hickie, I. B. (2010). Impaired MMN/P3a complex in first-episode psychosis: Cognitive and psychosocial associations. *Progress in Neuro-Psychopharmacology and Biological Psychiatry*, *34*(6), 822–829. https://doi.org/10.1016/j.pnpbp.2010.03.019

Higuchi, Y., Sumiyoshi, T., Seo, T., Miyanishi, T., Kawasaki, Y., & Suzuki, M. (2013). Mismatch negativity and cognitive performance for the prediction of psychosis in subjects with at-risk mental state. *PLoS ONE*, *8*(1), e54080. https://doi.org/10.1371/journal.pone.0054080

Hillebrand, A., & Barnes, G. R. (2002). A quantitative assessment of the sensitivity of whole-head MEG to activity in the adult human cortex. *NeuroImage*, *16*(3 I), 638–650. https://doi.org/10.1006/nimg.2002.1102

Hirayasu, Y., Shenton, M. E., Salisbury, D. F., Dickey, C. C., Fischer, I. A., Mazzoni, P., Kisler, T., Arakaki, H., Kwon, J. S., Anderson, J. E., Yurgelun-Todd, D., Tohen, M., & McCarley, R. W. (1998). Lower left temporal lobe MRI volumes in patients with first-episode schizophrenia compared with psychotic patients with first-episode affective disorder and normal subjects. *American Journal of Psychiatry*, *155*(10), 1384–1391. https://doi.org/10.1176/ajp.155.10.1384

Hochberger, W. C., Joshi, Y. B., Zhang, W., Thomas, M. L., Braff, D. L., Swerdlow, N. R., & Light, G. A. (2019). Decomposing the constituent oscillatory dynamics underlying mismatch negativity generation in schizophrenia: Distinct relationships to clinical and cognitive functioning. *International Journal of Psychophysiology*, *145*, 23–29. https://doi.org/10.1016/j.ijpsycho.2018.12.014

Hochberger, W. C., Thomas, M. L., Joshi, Y. B., Swerdlow, N. R., Braff, D. L., Gur, R. E., Gur, R. C., & Light, G. A. (2020). Deviation from expected cognitive ability is a core cognitive feature of schizophrenia related to neurophysiologic, clinical and psychosocial functioning. *Schizophrenia Research*, *215*, 300–307. https://doi.org/10.1016/j.schres.2019.10.011

Hollingshead, A. (1975). Four factor index of social status. *Yale Journal of Sociology*, *8*, 1–6.

Hua, J. P. Y., Roach, B. J., Ford, J. M., & Mathalon, D. H. (2023). Mismatch negativity and theta oscillations evoked by auditory deviance in early schizophrenia. *Biological Psychiatry: Cognitive Neuroscience and Neuroimaging*. in press. https://doi.org/10.1016/j.bpsc.2023.03.004

Javit, D. C., Steinschneider, M., Schroeder, C. E., Vaughan, H. G., & Arezzo, J. C. (1994). Detection of stimulus deviance within primate primary auditory cortex: Intracortical mechanisms of mismatch negativity (MMN) generation. *Brain Research*, *667*(2), 192–200. https://doi.org/10.1016/0006-8993(94)91496-6

Javitt, D. C., Shelley, A. M., & Ritter, W. (2000). Associated deficits in mismatch negativity generation and tone matching in schizophrenia. *Clinical Neurophysiology*, *111*(10), 1733–1737. https://doi.org/10.1016/S1388-2457(00)00377-1

Javitt, D. C., Steinschneider, M., Schroeder, C. E., & Arezzo, J. C. (1996). Role of cortical N-methyl-D-aspartate receptors in auditory sensory memory and mismatch negativity generation: Implications for schizophrenia. *Proceedings of the National Academy of Sciences of the United States of America*, *93*(21), 11962–11967. https://doi.org/10.1073/pnas.93.21.11962

Kasai, K., Shenton, M. E., Salisbury, D. F., Hirayasu, Y., Onitsuha, T., Spencer, M. H., Yurgelun-Todd, D. A., Kikinis, R., Jolesz, F. A., & McCarley, R. W. (2003). Progressive decrease of left Heschl gyrus and planum temporale gray matter volume in first-episode schizophrenia: A longitudinal magnetic resonance imaging study. *Archives of General Psychiatry*, *60*(8), 766–775. https://doi.org/10.1001/archpsyc.60.8.766

Kaur, M., Battisti, R. A., Ward, P. B., Ahmed, A., Hickie, I. B., & Hermens, D. F. (2011). MMN/P3a deficits in first episode psychosis: Comparing schizophrenia-spectrum and affective-spectrum subgroups. *Schizophrenia Research*, *130*(1–3), 203–209. https://doi.org/10.1016/j.schres.2011.03.025

Kawasaki, Y., Suzuki, M., Takahashi, T., Nohara, S., McGuire, P. K., Seto, H., & Kurachi, M. (2008). Anomalous cerebral asymmetry in patients with schizophrenia demonstrated by voxel-based morphometry. *Biological Psychiatry*, *63*(8), 793–800. https://doi.org/10.1016/j.biopsych.2007.08.008

Kay, S. R., Fiszbein, A., & Opler, L. A. (1987). The positive and negative syndrome scale (PANSS) for schizophrenia. *Schizophrenia Bulletin*, *13*(2), 261–276. https://doi.org/10.1093/schbul/13.2.261

Korvenoja, A., Kirveskari, E., Aronen, H. J., Avikainen, S., Brander, A., Huttunen, J., Ilmoniemi, R. J., Jääskeläinen, J. E., Kovala, T., Mäkelä, J. P., Salli, E., & Seppä, M. (2006). Sensorimotor cortex localization: Comparison of magnetoencephalography, functional MR imaging, and intraoperative cortical mapping. *Radiology*, *241*(1), 213–222. https://doi.org/10.1148/radiol.2411050796

Krishnan, A., & Gandour, J. T. (2009). The role of the auditory brainstem in processing linguistically-relevant pitch patterns. *Brain and Language*, *110*(3), 135–148. https://doi.org/10.1016/j.bandl.2009.03.005

Kropotov, J. D., Näätänen, R., Sevostianov, A. V., Alho, K., Reinikainen, K., & Kropotova, O. V. (1995). Mismatch negativity to auditory stimulus change recorded directly from the human temporal cortex. *Psychophysiology*, *32*(4), 418–422. https://doi.org/10.1111/j.1469-8986.1995.tb01226.x

Lakatos, P., O'Connell, M. N., Barczak, A., McGinnis, T., Neymotin, S., Schroeder, C. E., Smiley, J. F., & Javitt, D. C. (2020). The thalamocortical circuit of auditory mismatch negativity. *Biological Psychiatry*, *87*(8), 770–780. https://doi.org/10.1016/j.biopsych.2019.10.029

Lee, M., Sehatpour, P., Hoptman, M. J., Lakatos, P., Dias, E. C., Kantrowitz, J. T., Martinez, A. M., & Javitt, D. C. (2017). Neural mechanisms of mismatch negativity dysfunction in schizophrenia. *Molecular Psychiatry*, *22*(11), 1585–1593. https://doi.org/10.1038/mp.2017.3

Light, G. A., & Braff, D. L. (2005). Mismatch negativity deficits are associated with poor functioning in schizophrenia patients. *Archives of General Psychiatry*, *62*(2), 127–136. https://doi.org/10.1001/archpsyc.62.2.127

Light, G. A., & Näätänen, R. (2013). Mismatch negativity is a breakthrough biomarker for understanding and treating psychotic disorders. *Proceedings of the National Academy of Sciences of the United States of America*, *110*(38), 15175–15176. https://doi.org/10.1073/pnas.1313287110

Lin, F. H., Witzel, T., Ahlfors, S. P., Stufflebeam, S. M., Belliveau, J. W., & Hämäläinen, M. S. (2006). Assessing and improving the spatial accuracy in MEG source localization by depth-weighted minimum-norm estimates. *NeuroImage*, *31*(1), 160–171. https://doi.org/10.1016/j.neuroimage.2005.11.054

Magno, E., Yeap, S., Thakore, J. H., Garavan, H., de Sanctis, P., & Foxe, J. J. (2008). Are auditory-evoked frequency and duration mismatch negativity deficits endophenotypic for schizophrenia? High-density electrical mapping in clinically unaffected first-degree relatives and first-episode and chronic schizophrenia. *Biological Psychiatry*, *64*(5), 385–391. https://doi.org/10.1016/j.biopsych.2008.03.019

Marinkovic, K., Cox, B., Reid, K., & Halgren, E. (2004). Head position in the MEG helmet affects the sensitivity to anterior sources. *Neurology and Clinical Neurophysiology*, *2004*, 30.

May, P. J. C., & Tiitinen, H. (2010). Mismatch negativity (MMN), the deviance-elicited auditory deflection, explained. *Psychophysiology*, *47*(1), 66–122. https://doi.org/10.1111/j.1469-8986.2009.00856.x

Medani, T., Garcia-Prieto, J., Tadel, F., Schrader, S., Antonakakis, M., Joshi, A. A., Engwer, C., Wolters, C. H., Mosher, J. C., & Leahy, R. M. (2021). Realistic head modeling of electromagnetic brain activity: an integrated Brainstorm-DUNEuro pipeline from MRI data to the FEM solutions. https://doi.org/10.1117/12.2580935

Merchant, H., Harrington, D. L., & Meck, W. H. (2013). Neural basis of the perception and estimation of time. In. *Annual Review of Neuroscience*, *36*, 313–336. https://doi.org/10.1146/annurev-neuro-062012-170349

Michie, P. T. (2001). What has MMN revealed about the auditory system in schizophrenia? *International Journal of Psychophysiology*, *42*(2), 177–194. https://doi.org/10.1016/S0167-8760(01)00166-0

Mohn-Haugen, C. R., Mohn, C., Larøi, F., Teigset, C. M., Øie, M. G., & Rund, B. R. (2022). A systematic review of premorbid cognitive functioning and its timing of onset in schizophrenia spectrum disorders. *Schizophrenia Research: Cognition*, *28*, 100246. https://doi.org/10.1016/j.scog.2022.100246

Molholm, S., Martinez, A., Ritter, W., Javitt, D. C., & Foxe, J. J. (2005). The neural circuitry of pre-attentive auditory change-detection: An fMRI study of pitch and duration mismatch negativity generators. *Cerebral Cortex*, *15*(5), 545–551. https://doi.org/10.1093/cercor/bhh155

Murphy, T. K., Haigh, S. M., Coffman, B. A., & Salisbury, D. F. (2020). Mismatch negativity and impaired social functioning in long-term and in first episode schizophrenia spectrum psychosis. *Frontiers in Psychiatry*, *11*, 544. https://doi.org/10.3389/fpsyt.2020.00544

Näätänen, R. (1990). The role of attention in auditory information processing as revealed by event-related potentials and other brain measures of cognitive function. *Behavioral and Brain Sciences*, *13*(2), 201–233. https://doi.org/10.1017/S0140525X00078407

Näätänen, R., Gaillard, A. W. K., & Mäntysalo, S. (1978). Early selective-attention effect on evoked potential reinterpreted. *Acta Psychologica*, *42*(4), 313–329. https://doi.org/10.1016/0001-6918(78)90006-9

Näätänen, R., Paavilainen, P., Rinne, T., & Alho, K. (2007). The mismatch negativity (MMN) in basic research of central auditory processing: A review. *Clinical Neurophysiology*, *118*(12), 2544–2590. https://doi.org/10.1016/j.clinph.2007.04.026

Näätänen, R., Teder, W., Alho, K., & Lavikainen, J. (1992). Auditory attention and selective input modulation: A topographical ERP study. *Neuroreport*, *3*(6), 493–496. https://doi.org/10.1097/00001756-199206000-00009

Näätänen, R., Todd, J., & Schall, U. (2016). Mismatch negativity (MMN) as biomarker predicting psychosis in clinically at-risk individuals. *Biological Psychology*, *116*, 36–40. https://doi.org/10.1016/j.biopsycho.2015.10.010

Nuechterlein, K. H., Green, M. F., Kern, R. S., Baade, L. E., Barch, D. M., Cohen, J. D., Essock, S., Fenton, W. S., Frese, F. J., Gold, J. M., Goldberg, T., Heaton, R. K., Keefe, R. S. E., Kraemer, H., Mesholam-Gately, R., Seidman, L. J., Stover, E., Weinberger, D. R., Young, A. S., ... Marder, S. R. (2008). The MATRICS consensus cognitive battery, part 1: Test selection, reliability, and validity. *American Journal of Psychiatry*, *165*(2), 203–213. https://doi.org/10.1176/appi.ajp.2007.07010042

Oades, R. D., Wild-Wall, N., Juran, S. A., Sachsse, J., Oknina, L. B., & Röpcke, B. (2006). Auditory change detection in schizophrenia: Sources of activity, related neuropsychological function and symptoms in patients with a first episode in adolescence, and patients 14 years after an adolescent illness-onset. *BMC Psychiatry*, *6*, 7. https://doi.org/10.1186/1471-244X-6-7

Olney, J. W., Newcomer, J. W., & Farber, N. B. (1999). NMDA receptor hypofunction model of schizophrenia. *Journal of Psychiatric Research*, *33*(6), 523–533. https://doi.org/10.1016/S0022-3956(99)00029-1

Park, H. J., Kwon, J. S., Youn, T., Pae, J. S., Kim, J. J., Kim, M. S., & Ha, K. S. (2002). Statistical parametric mapping of LORETA using high density EEG and individual MRI: Application to mismatch negativities in schizophrenia. *Human Brain Mapping*, *17*(3), 168–178. https://doi.org/10.1002/hbm.10059

Rammsayer, T. (1990). Temporal discrimination in schizophrenic and affective disorders: Evidence for a dopamine-dependent internal clock. *International Journal of Neuroscience*, *53*(2–4), 111–120. https://doi.org/10.3109/00207459008986593

Randau, M., Oranje, B., Miyakoshi, M., Makeig, S., Fagerlund, B., Glenthøj, B., & Bak, N. (2019). Attenuated mismatch negativity in patients with first-episode antipsychotic-naive schizophrenia using a source-resolved method. *NeuroImage: Clinical*, *22*, 101760. https://doi.org/10.1016/j.nicl.2019.101760

Rasser, P. E., Schall, U., Todd, J., Michie, P. T., Ward, P. B., Johnston, P., Helmbold, K., Case, V., Søyland, A., Tooney, P. A., & Thompson, P. M. (2011). Gray matter deficits, mismatch negativity, and outcomes in schizophrenia. *Schizophrenia Bulletin*, *37*(1), 131–140. https://doi.org/10.1093/schbul/sbp060

Ress, D., & Chandrasekaran, B. (2013). Tonotopic organization in the depth of human inferior colliculus. *Frontiers in Human Neuroscience*, *7*, 586. https://doi.org/10.3389/fnhum.2013.00586

Rinne, T., Alho, K., Ilmoniemi, R. J., Virtanen, J., & Näätänen, R. (2000). Separate time behaviors of the temporal and frontal mismatch negativity sources. *NeuroImage*, *12*(1), 14–19. https://doi.org/10.1006/nimg.2000.0591

Rissling, A. J., Miyakoshi, M., Sugar, C. A., Braff, D. L., Makeig, S., & Light, G. A. (2014). Cortical substrates and functional correlates of auditory deviance processing deficits in schizophrenia. *NeuroImage: Clinical*, *6*, 424–437. https://doi.org/10.1016/j.nicl.2014.09.006

Rosburg, T., Trautner, P., Dietl, T., Korzyukov, O. A., Boutros, N. N., Schaller, C., Elger, C. E., & Kurthen, M. (2005). Subdural recordings of the mismatch negativity (MMN) in patients with focal epilepsy. *Brain*, *128*(4), 819–828. https://doi.org/10.1093/brain/awh442

Salisbury, D. F., Kuroki, N., Kasai, K., Shenton, M. E., & McCarley, R. W. (2007). Progressive and interrelated functional and structural evidence of post-onset brain reduction in schizophrenia. *Archives of General Psychiatry*, *64*(5), 521–529. https://doi.org/10.1001/archpsyc.64.5.521

Salisbury, D. F., Polizzotto, N. R., Nestor, P. G., Haigh, S. M., Koehler, J., & McCarley, R. W. (2017). Pitch and duration mismatch negativity and premorbid intellect in the first hospitalized schizophrenia spectrum. *Schizophrenia Bulletin*, *43*(2), sbw074–sbw416. https://doi.org/10.1093/schbul/sbw074

Salisbury, D. F., Shafer, A. R., Murphy, T. K., Haigh, S. M., & Coffman, B. A. (2020). Pitch and duration mismatch negativity and Heschl's gyrus volume in first-episode schizophrenia-spectrum individuals. *Clinical EEG and Neuroscience*, *51*(6), 359–364. https://doi.org/10.1177/1550059420914214

Salisbury, D. F., Shenton, M. E., Griggs, C. B., Bonner-Jackson, A., & McCarley, R. W. (2002). Mismatch negativity in chronic schizophrenia and first-episode schizophrenia. *Archives of General Psychiatry*, *59*(8), 686. https://doi.org/10.1001/archpsyc.59.8.686

Schrader, S., Westhoff, A., Piastra, M. C., Miinalainen, T., Pursiainen, S., Vorwerk, J., Brinck, H., Wolters, C. H., & Engwer, C. (2021). DUNEuro - a software toolbox for forward modeling in bioelectromagnetism. *PLoS ONE*, *16*, e0252431. https://doi.org/10.1371/journal.pone.0252431

Shelley, A. M., Ward, P. B., Catts, S., Michie, P. T., Andrews, S., & McConaghy, N. (1991). Mismatch negativity: An index of a preattentive processing deficit in schizophrenia. *Biological Psychiatry*, *30*(10), 1059–1062. https://doi.org/10.1016/0006-3223(91)90126-7

Shin, K. S., Kim, J. S., Kang, D. H., Koh, Y., Choi, J. S., O'Donnell, B. F., Chung, C. K., & Kwon, J. S. (2009). Pre-attentive auditory processing in ultra-high-risk for schizophrenia with magnetoencephalography. *Biological Psychiatry*, *65*(12), 1071–1078. https://doi.org/10.1016/j.biopsych.2008.12.024

Shiramatsu, T. I., Kanzaki, R., & Takahashi, H. (2013). Cortical mapping of mismatch negativity with deviance detection property in rat. *PLoS ONE*, *8*(12), e82663. https://doi.org/10.1371/journal.pone.0082663

Smiley, J. F., Hackett, T. A., Preuss, T. M., Bleiwas, C., Figarsky, K., Mann, J. J., Rosoklija, G., Javitt, D. C., & Dwork, A. J. (2013). Hemispheric asymmetry of primary auditory cortex and Heschl's gyrus in schizophrenia and nonpsychiatric brains. *Psychiatry Research - Neuroimaging*, *214*(3), 435–443. https://doi.org/10.1016/j.pscychresns.2013.08.009

Smiley, J. F., Rosoklija, G., Mancevski, B., Mann, J. J., Dwork, A. J., & Javitt, D. C. (2009). Altered volume and hemispheric asymmetry of the superficial cortical layers in the schizophrenia planum temporale. *European Journal of Neuroscience*, *30*(3), 449–463. https://doi.org/10.1111/j.1460-9568.2009.06838.x

Sweet, R. A., Henteleff, R. A., Zhang, W., Sampson, A. R., & Lewis, D. A. (2009). Reduced dendritic spine density in auditory cortex of subjects with schizophrenia. *Neuropsychopharmacology*, *34*(2), 374–389. https://doi.org/10.1038/npp.2008.67

Tadel, F., Baillet, S., Mosher, J. C., Pantazis, D., & Leahy, R. M. (2011). Brainstorm: A user-friendly application for MEG/EEG analysis. *Computational Intelligence and Neuroscience*, *2011*, 879716. https://doi.org/10.1155/2011/879716

Taulu, S., & Simola, J. (2006). Spatiotemporal signal space separation method for rejecting nearby interference in MEG measurements. *Physics in Medicine and Biology*, *51*(7), 1759–1768. https://doi.org/10.1088/0031-9155/51/7/008

Taulu, S., Simola, J., & Kajola, M. (2004). Clinical applications of the signal space separation method. *International Congress Series*, *1270*(C), 32–37. https://doi.org/10.1016/j.ics.2004.05.004

Thompson, P. M., Vidal, C., Giedd, J. N., Gochman, P., Blumenthal, J., Nicolson, R., Toga, A. W., & Rapoport, J. L. (2001). Mapping adolescent brain change reveals dynamic wave of accelerated gray matter loss in very early-onset schizophrenia. *Proceedings of the National Academy of Sciences of the United States of America*, *98*(20), 11650–11655. https://doi.org/10.1073/pnas.201243998

Todd, J., Harms, L., Schall, U., & Michie, P. T. (2013). Mismatch negativity: Translating the potential. *Frontiers in Psychiatry*, *4*, 171. https://doi.org/10.3389/fpsyt.2013.00171

Todd, J., Howard, Z., Auksztulewicz, R., & Salisbury, D. (2022). Computational modeling of oddball sequence processing exposes common and differential auditory network changes in first-episode schizophrenia-spectrum disorders and schizophrenia. *Schizophrenia Bulletin*, *49*(2), 407–416.

Todd, J., Michie, P. T., Budd, T. W., Rock, D., & Jablensky, A. V. (2000). Auditory sensory memory in schizophrenia: Inadequate trace formation? *Psychiatry Research*, *96*, 99–115. https://doi.org/10.1016/S0165-1781(00)00205-5

Todd, J., Michie, P. T., & Jablensky, A. V. (2003). Association between reduced duration mismatch negativity (MMN) and raised temporal discrimination thresholds in schizophrenia. *Clinical Neurophysiology*, *114*(11), 2061–2070. https://doi.org/10.1016/S1388-2457(03)00246-3

Todd, J., Michie, P. T., Schall, U., Karayanidis, F., Yabe, H., & Näätänen, R. (2008). Deviant matters: Duration, frequency, and intensity deviants reveal different patterns of mismatch negativity reduction in early and late schizophrenia. *Biological Psychiatry*, *63*(1), 58–64. https://doi.org/10.1016/j.biopsych.2007.02.016

Todd, J., Michie, P. T., Schall, U., Ward, P. B., & Catts, S. V. (2012). Mismatch negativity (MMN) reduction in schizophrenia-impaired prediction-error generation, estimation or salience? In. *International Journal of Psychophysiology*, *83*(2), 222–231. https://doi.org/10.1016/j.ijpsycho.2011.10.003

Umbricht, D., & Krljes, S. (2005). Mismatch negativity in schizophrenia: A meta-analysis. *Schizophrenia Research*, *76*(1), 1–23. https://doi.org/10.1016/j.schres.2004.12.002

Valkonen-Korhonen, M., Purhonen, M., Tarkka, I. M., Sipilä, P., Partanen, J., Karhu, J., & Lehtonen, J. (2003). Altered auditory processing in acutely psychotic never-medicated first-episode patients. *Cognitive Brain Research*, *17*(3), 747–758. https://doi.org/10.1016/S0926-6410(03)00199-X

Valt, C., Quarto, T., Tavella, A., Romanelli, F., Fazio, L., Arcara, G., Altamura, M., Barrasso, G., Bellomo, A., & Blasi, G. (2022). Reduced magnetic mismatch negativity: A shared deficit in psychosis and related risk. *Psychological Medicine*, 1–9. https://doi.org/10.1017/S003329172200321X

Winkler, I. (2007). Interpreting the mismatch negativity. *Journal of Psychophysiology*, *21*(3–4), 147–163. https://doi.org/10.1027/0269-8803.21.34.147

Wynn, J. K., Sugar, C., Horan, W. P., Kern, R., & Green, M. F. (2010). Mismatch negativity, social cognition, and functioning in schizophrenia patients. *Biological Psychiatry*, *67*(10), 940–947. https://doi.org/10.1016/j.biopsych.2009.11.024

Youn, T., Park, H. J., Kim, J. J., Kim, M. S., & Kwon, J. S. (2003). Altered hemispheric asymmetry and positive symptoms in schizophrenia: Equivalent current dipole of auditory mismatch negativity. *Schizophrenia Research*, *59*(2–3), 253–260. https://doi.org/10.1016/S0920-9964(02)00154-8

Yvert, B., Fischer, C., Guénot, M., Krolak-Salmon, P., Isnard, J., & Pernier, J. (2002). Simultaneous intracerebral EEG recordings of early auditory thalamic and cortical activity in human. *European Journal of Neuroscience*, *16*(6), 1146–1150. https://doi.org/10.1046/j.1460-9568.2002.02162.x

Zatorre, R. J., & Belin, P. (2001). Spectral and temporal processing in human auditory cortex. *Cerebral Cortex*, *11*(10), 946–953. https://doi.org/10.1093/cercor/11.10.946

Zatorre, R. J., Belin, P., & Penhune, V. B. (2002). Structure and function of auditory cortex: Music and speech. *Trends in Cognitive Sciences*, *6*(1), 37–46. https://doi.org/10.1016/S1364-6613(00)01816-7

SUPPORTING INFORMATION

Additional supporting information can be found online in the Supporting Information section at the end of this article.

How to cite this article: López-Caballero, F., Curtis, M., Coffman, B. A., & Salisbury, D. F. (2024). Is source-resolved magnetoencephalographic mismatch negativity a viable biomarker for early psychosis? *European Journal of Neuroscience*, *59*(8), 1889–1906. https://doi.org/10.1111/ejn.16107